Next Generation Packaging Architectures for Highly Integrated Wireless Systems

J. Laskar, M. Tentzeris, A. Sutono, H. Liang, N.Bushyager and K. Lim

etentze@ece.gatech.edu

Packaging Research Center
School of Electrical and Computer Engineering
Georgia Institute of Technology
Atlanta, GA 30332-0250

ABSTRACT

We present the development and characterization of three critical technologies for wireless communication packaging architectures. In this paper, we include the design, implementation and measurement results of embedded components for multi-chip-modules (MCM) and micromachined planar antennas. In addition, an optimized digital Pin Grid Array (PGA) package has been built and demonstrates suitable application for wireless packaging architectures.

INTRODUCTION

Multi-layer integrated components, optimized PGA technology for microwave packaging, and micromachining technique are critical to meet the cost and performance requirement of highly integrated wireless systems. Embedded components [1] and micromachining [2] technology allow a higher level of integration in the development of a wireless transceiver system. They offer the potential for saving the assembly time and cost by considerably reducing the MMIC real estate and the amount of discrete elements used in the module. Three dimensional lumped element embedded inductors [3,5] have demonstrated superior Q to those implemented on chip for applications to 5 GHz. Various micromachined structures [4] show applicability in high frequency communication systems. In this paper, we present the design, implementation and measurements of a three-dimensional Bluetooth filter and a micromachined patch antenna as examples of compact embedded components and easily integrable efficient radiating structures In addition, a conventional low-cost digital Pin Grid Array packaging technology has been modified and optimized for microwave packaging solution. Such topology, originally developed by Agilent Technologies is referred to as Multichip Integral-Substrate PGA Package Solution (MIPPS) [6]. A test structure consisting of a 90 degrees transition from a microstrip line to a coaxial line has been fabricated and measured to assess the package performance.

PACKAGING TOPOLOGIES

Figure 1 shows the three-dimensional view of a 2.4 GHz LTCC bluetooth filter implemented in lumped element stripline topology where all the components are buried between two ground planes separated by six layers of dielectric (21.6 mils). Layer 6 and 0 are the ground plane of the filter. The filter consists of two LC resonators whose inductors and capacitors are implemented by the two overlapping strips on layer 5 and 4, respectively and the two plates on layer 1 right on top of the bottom ground plane. Two series capacitors are formed between layer 5 and 4 for impedance matching purpose. A middle series vertically interdigitated capacitor formed the plates by layer 3,2, and 1 is used to set the null at the image frequency of about 2.1 GHz. The photograph of the fabricated LTCC filters is shown in Figure 2. In the actual transceiver, this

filter can be easily integrated on the LTCC board where the entire receiver is built.

Figure 3 shows the topology of a K-band micromachined patch antenna that was introduced in [4] demonstrating an increase in the bandwidth by a factor close to 2. It can be built on Si or GaAs, or other substrates that facilitate a higher level of integration with the rest of the wireless system. As indicated in Figure 3, the substrate material underneath the antenna is removed by selective etching. Even 1:1 air-substrate thickness ratio can provide an ε_{eff} quite close to 1. The newly created micromachined cavity supresses the surface waves and decreases the dielectric loss. In addition, it was reported that the radiation efficiency is increased from 56% to 73% and the radiation pattern is much smoother.

The MIPPS package mainly consists of a metal base plate, a ceramic substrate, and a lid. In the metal base plate, a recess is made to serve as a housing for the microcircuits which are built on a ceramic substrate. Gold pins are vertically connected to the microstrip to form the RF transitions with the microcircuits. A circular area of metal on the backside of the substrate is etched to provide some clearance between the pin and the ground plane of the microstrip,. The vertical pins come out the backside of the alumina and go through machined holes in the metal baseplate forming a short airline coaxial section. The pins are located such that convenient assembly of circuit board and testing are made possible. A 90 degrees microstrip to stripline transition test structure as shown in Figure 4 has been fabricated to assess the package performance.

SIMULATION TECHNIQUES

The Finite-Difference Time-Domain (FDTD) technique has been used for the full-wave modeling of the packaging structures. FDTD discretizes Maxwell's Curl equations and creates grids with interlaced positioning of the electromagnetic field components. The U-PML absorbers have been utilized to terminate the grid. In addition, the 0-th and 1-st order Haar wavelets have been enhanced in areas of high local geometrical detail leading to 3D schemes [7]. Wavelets have been also placed at locations where the EM fields have had significant values, creating a space- and time- adaptive dense mesh in regions of strong field variations, while maintaining a much coarser mesh elsewhere. In this way, the computational requirements have been minimized and the simulations have been performed with cell sizes close to the Nyquist limit. In addition, the unique MRTD capability of multidielectric intracell modeling allowed for the fast and accurate design especially of the micromachined structures.

EXPERIMENTAL RESULTS

The overall size of the Bluetooth filter is 5.2 mm x 3 mm x 0.5 mm with the measurement pads and 3.8 mm x 2.4 mm x 0.5 mm without measurement pads. Figure 5 shows the measured data of the initial filter prototype superimposed with the electromagnetic simulation results using a commercial Method of Moments (MoM) simulator [8] and a custom simulator implementing the Partial Element Equivalent Circuit (PEEC) algorithm [9]. The measurement and simulation results exhibit a good correlation. The insertion loss of the filter at the center frequency of 2.38 GHz is 3 dB with the return loss at the center frequency and a bandwidth of 20 dB and 270 MHz, respectively.

The micromachined antenna structure has been simulated for different t_{air}/t ratios ranging from 0.5 to 0.9 and results demonstrate a bandwidth spreading by a factor of 1.8 that saturates above 0.82. FDTD and MRTD results investigating the effect of these ratios on the radiation pattern and the return loss will be presented in the conference for designs on Si around 1.9GHz and 5.8GHz.

Figure 6 shows the measured and simulated return loss performance of the MIPPS test structure. The simulation was performed

using a commercial Finite Element simulator [10]. The measured return loss is better than 20 dB at 20 GHz showing good agreement between measured and simulated results and demonstrating better performance than the first generation prototype.

CONCLUSION

We have presented the design, implementation, optimization and characterization 3D embedded bluetooth filter, micromachined planar antenna and advanced PGA packaging structures. These three examples represent the next generation packaging topologies suitable for the implementation of a highly integrated wireless systems. Experimental data have been presented and demonstrate usability in various wireless applications.

ACKNOWLEDGMENT

The authors would like to acknowledge NSF Packaging Research Center for their support. We also would like to thank Dick Smith and Mike Ehlert from National Semiconductor, Heidi Barnes and Don Estrich from Agilent Technologies for fabricating prototype test structures.

References

[1] J. Rector, "Economic and Technical Viability of Integral Passives," *1998 IEEE ECTC Digest*, pp.218-224.

[2] L.P.B. Katehi, G. M. Rebeiz, C.T. Nguyen, "MEMS and Si-micromachined components for low-power, high-frequency communications systems," *IEEE MTT-S Digest*, vol.1, pp.331-333, June 1998, Baltimore, MD.

[3] R.L. Brown, P.W. Polinski, "The Integration of Passive Components Into MCMs Using Advanced Low-Temperature Cofired Ceramics," *1993 International Journal of Microcircuit and Electronic Packaging, v.16 n.4*, pp.328-338.

[4] I.Papapolymerou, R.F.Drayton, L.P.B.Katehi, "Micromachined Patch Antennas," *IEEE Transactions on Antennas and Propagation*, vol.46, pp.275-283, Feb.1998.

[5] A. Sutono, A.Pham, J. Laskar, and W.R. Smith, "Development of Three Dimensional Ceramic-Based MCM Inductors for Hybrid RF/Microwave Applications," *IEEE-RFIC Sym.Dig, pp*175-178, Anaheim, CA, June 1999.

[6] L.R.Dove, M.L.Guth, D.B.Nicholson, "A Low-Cost RF Multichip Module Packaging Family", *The Hewlett-Packard Journal*, pp53-60, Aug. 1998

[7] L.P.B.Katehi, J.Harvey and E.Tentzeris, "TimeDomain Analysis Using Multiresolution Expansions",Invited Chapter, "Advances in Computational Electrodynamics", edited by A.Taflove,pp.111-162, Artech House, 1998

[8] EM User Manual, Sonnet Software Inc., Liverpool, NY.

[9] A.E. Ruehli, "Equivalent Circuit Models for Three Dimensional Multiconductor Systems," *IEEE Trans. Microwave Theory Tech.*, vol.MTT-22, no.3, March 1974

[10]HP 85180 High-Frequency Structure Simulator Version 5.4, 1999

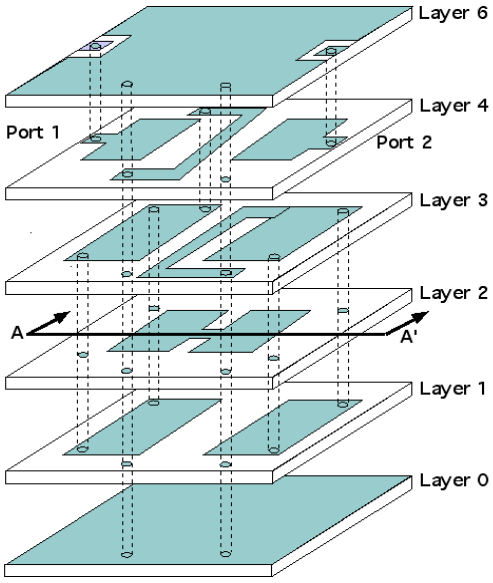

Figure 1. Multi-layer integrated filter topology.

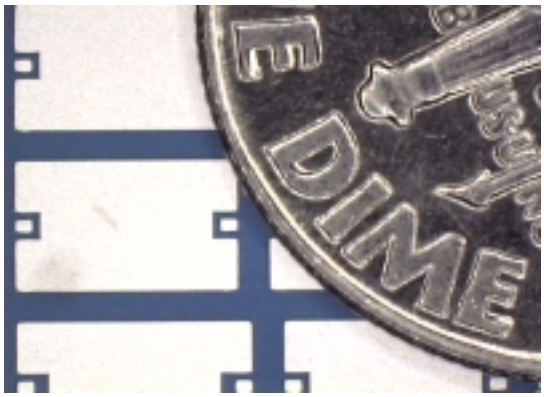

Figure 2. Photograph of Bluetooth image reject filters.

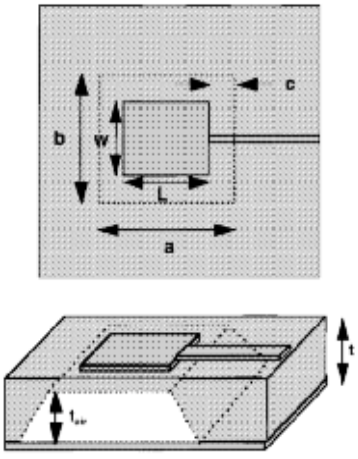

Figure 3. Micromachined antenna schematic.

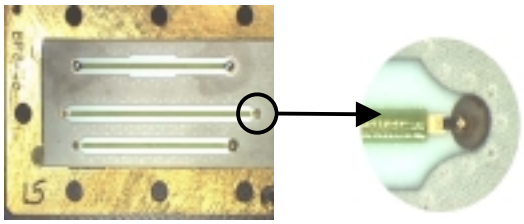

Figure 4. Photograph of MIPPS transition.

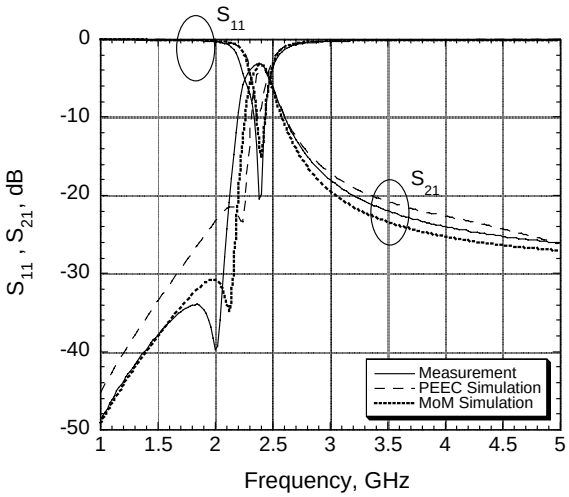

Figure 5. Experimental result of the LTCC Bluetooth filter.

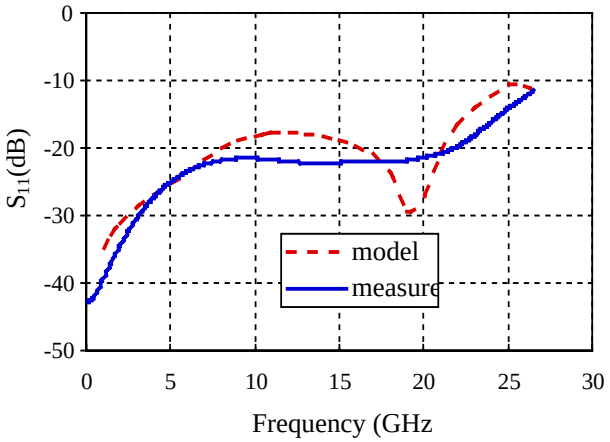

Figure 6. Return loss performance of the MIPPS transition.